

Dynamic Analysis and Seismic Responses of Industrial Rack Structures with Perforated Cold-formed Steel Columns using Line Elements

Wen-Long Gao¹, Si-Wei Liu², Teoman Pekoz³, Ronald D. Ziemian⁴ and James Crews⁵

Abstract

Industrial rack structures with perforated cold-formed steel columns and braces are extensively used in high seismic intensity regions, whose dynamic responses under transient excitations should be carefully evaluated for ensuring structural safety. Nevertheless, it is difficult to robustly analyze such structural systems comprised of monosymmetrical open-section members, mostly because of their complicated cross-section shapes with non-coincidence of shear centre and centroid for inducing the Wagner's effects and complex buckling modes. Until now, there was no free and easy-to-use computer program available for frames with considering these features, especially for seismic design of industrial rack structures. Recent research, developing efficient line element formulations, has made substantial progress in simulating the buckling behavior of nonsymmetrical section members for both static and dynamic loads. These new element formulations have been implemented into a newer version of the educational analysis software MASTAN2-v5.1, which is introduced for the transient analysis of the industrial rack with perforated cold-formed steel columns for evaluating their seismic responses. The numerical algorithms, including mathematical derivations, are illustrated in brief. An efficient method for considering perforations on the column is proposed, where the steel plate thickness is reduced for such considerations. Validation examples are given, where the numerical method using shell elements are used to generate the benchmark solutions. In this study, some additional features such as the treatment of thin-walled perforated columns, axially and flexural semi-rigid connections are explored. The common industrial rack structures are studied for evaluating the dynamic responses under typical earthquake excitations, that can provide useful information for their applications in high seismic intensity regions.

1. Introduction

Steel storage rack structures, with various structural forms for suiting different applications, are widely used in logistics and the other related industries. As such, some particular requirements [1, 2] are needed for the design of rack structures according to their actual application conditions. Taking a typical prefabricated pallet rack structure as an example (Figure 1), its structural behavior in the down-aisle direction appears to be similar to the moment-resistance frame (MRF), however, in the along-aisle direction, the structural behavior is significantly different to the MRF. Moreover, these rack structures are usually fabricated by the mono-symmetrical cold-formed steel sections for columns and braces, which are usually susceptible to buckle in the complicated modes, especially under the complex loading conditions. (Figure 2) Therefore, the stability analysis associated with the prediction on the buckling strength of these members is vital for the successful design

and has been studied by a number of researchers during the past decades. [4-9] These attentions are mostly focused on the static analysis, while the dynamic analysis for these members and the storage racks are still limited. To this end, this paper focuses on studying the dynamic responses under transient excitations of the industrial rack structures with perforated cold-formed steel columns and braces for seismic design.

The members with mono-symmetrical thin-walled sections are commonly used in the industrial storage racks, which are weak in resisting torsion. The behavior of these nonsymmetrical sections is complex because the shear center does not coincide with its centroid. In addition, the buckling behavior of these members is further complicated by local and distortional buckling and the perforations that facilitate the connections of the frames. Current engineering practice mainly relies on the frame analysis based on the doubly symmetrical section assumption [9, 10] which could

¹ MPhil Student, Sun Yat-Sen University, gaowlong3@mail2.sysu.edu.cn

² Associate Professor, Sun Yat-Sen University, siwei.liu@connect.polyu.hk

³ Emeritus Professor, Cornell University, tp26@cornell.edu

⁴ Professor, Bucknell University, ziemian@bucknell.edu

⁵ Engineer, UNARCO Material Handling, Inc., JCrews@UNARCORACK.com

be inaccurate when evaluating the global buckling strength of an unsymmetrical section member. The structural behavior of a cantilever beam analyzed by different approaches are schematically illustrated in Figure 3. A study

showing the importance of proper modeling of nonsymmetrical members using appropriate elements can be found in the reference [21].



Figure 1: An industrial rack structure with perforated cold-formed steel columns

Different from the conventional steel columns, the columns in racks are usually perforated on the web along the member length for easing the difficulties in connecting the horizontal beams of being convenient in the erection, as illustrated in Figure 3 below. As studied by Zhao et al. [12, 13], the perforations on the column significantly affect the buckling modes associated with the member strength. Several experimental investigations [14-17] have been conducted for examining the buckling behaviors of the perforated columns, revealing that the buckling strengths of the intermediate length columns are significantly affected by the perforations. However, the buckling modes of such columns are intricate because of the coupling of local and global buckling modes, further complicating the proper calculation for their buckling strengths. Recently, Casafont et al. [18] employed the Finite Strip Method (FSM) [19] and proposed a method by reducing the plate thickness for computing the buckling strength of the perforated cold-formed steel columns, but this method is only suitable for the single-member design under static loads. Therefore, there is a need for developing an analysis of the columns with perforations, being suitable for both the static and the dynamic analyses.

Recently, an efficient line element formulation is developed by the authors of the paper [20, 21], which can simulate the buckling behavior of nonsymmetrical section members for

both static and dynamic loads. These new element formulations have been implemented into a newer version of the educational analysis software MASTAN2-v5.1 [22], which is introduced for transient analysis of the industrial rack with perforated cold-formed steel columns for evaluating its seismic responses. This will be introduced in brief in this paper, and several examples are given to illustrate the dynamic analyses of the steel pallet racks under seismic excitations.

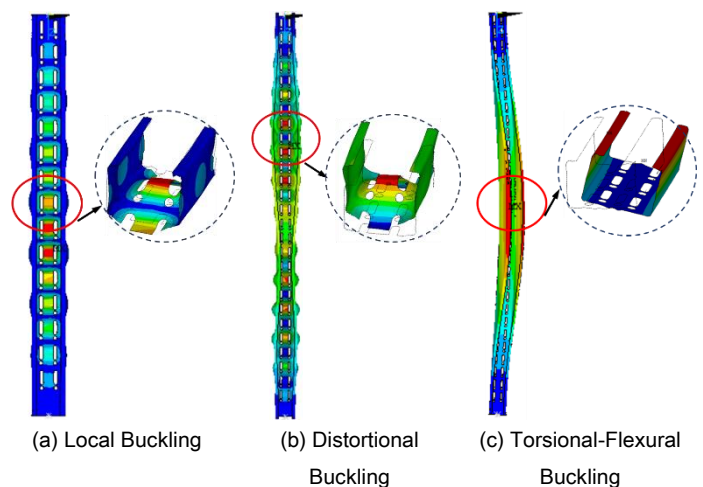
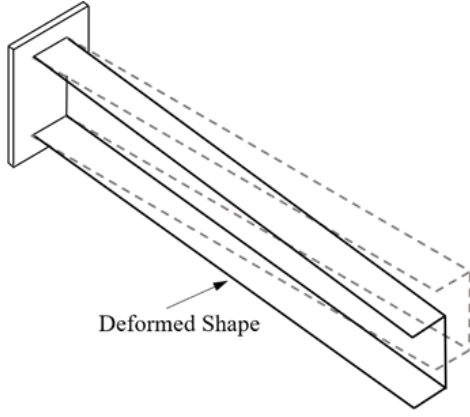
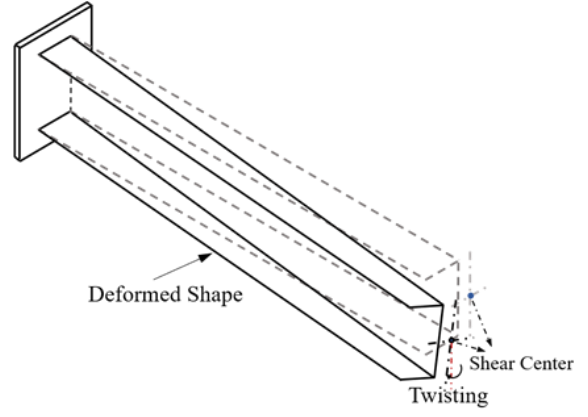


Figure 2 Types of buckling of perforated column



(a) Using doubly-symmetrical section assumption – No twisting



(b) Using non-symmetrical section assumption – Twisting

Figure 3 Deformation shapes by different analysis approaches

2. Modeling of Perforated Cold-formed steel columns

The effect of perforations on the buckling loads are accounted for by assuming the reduced thickness strips where the perforations are located as shown in Figure 4. The concept of reduced thickness strips is described in the reference [6]. The reduced thicknesses of strips were calculated as follows.

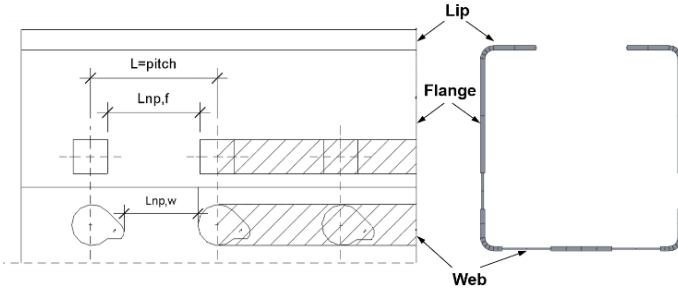


Figure 4 Reduced thickness strips to account for perforations

For the global buckling calculations, the plate the reduced strip thickness is computed by,

$$t_{g,w} = k_g t \left(\frac{L_{np,w}}{L} \right) \quad (1)$$

$$t_{g,f} = k_g t \left(\frac{L_{np,f}}{L} \right) \quad (2)$$

where $t_{g,w}$ and $t_{g,f}$ are thicknesses of the strips containing web and flange perforations $k_g = 0.6$.

For determining the distortional buckling value, the plate the reduced strip thickness is obtained by,

$$t_{d,w} = k_d t \left(\frac{L_{np,w}}{L} \right)^{1/3} \quad (3)$$

$$t_{d,f} = k_d t \left(\frac{L_{np,f}}{L} \right)^{1/3} \quad (4)$$

in which, $k_d = 0.8$ for computing the elastic distortional buckling loads.

3. Line Element with Nonsymmetric Sections

The major feature of the frame analysis in MASTAN2-v5.1 is its element being capable of accurately simulating the global buckling behaviors of nonsymmetrical section members in terms of axial-torsional, flexural-torsional and axial flexural buckling. The element formulations have been extensively verified by numbers of examples and verified by several researchers independently from University of Wisconsin–Madison, Polytechnic University of Milan and Hong Kong Polytechnic University and so on. More details regarding to the line-element can be found in the references [1, 2], which can be summarized as follows. As shown in Figure 7, this element includes the warping degree-of-freedom (DOF) and the element formulation is established based on the section principal local axis system.

- The element formulations are derived for arbitrarily shaped cross-sections regardless of open-, closed- or multicellular shapes.
- The Wagner effects and the non-coincidence of shear-center and centroid are directly modelled.
- Large deflection is allowed by using the Updated-Lagrangian (UL) method.
- The major- (strongest) and minor- (weakest) principal section-axes are automatically considered.

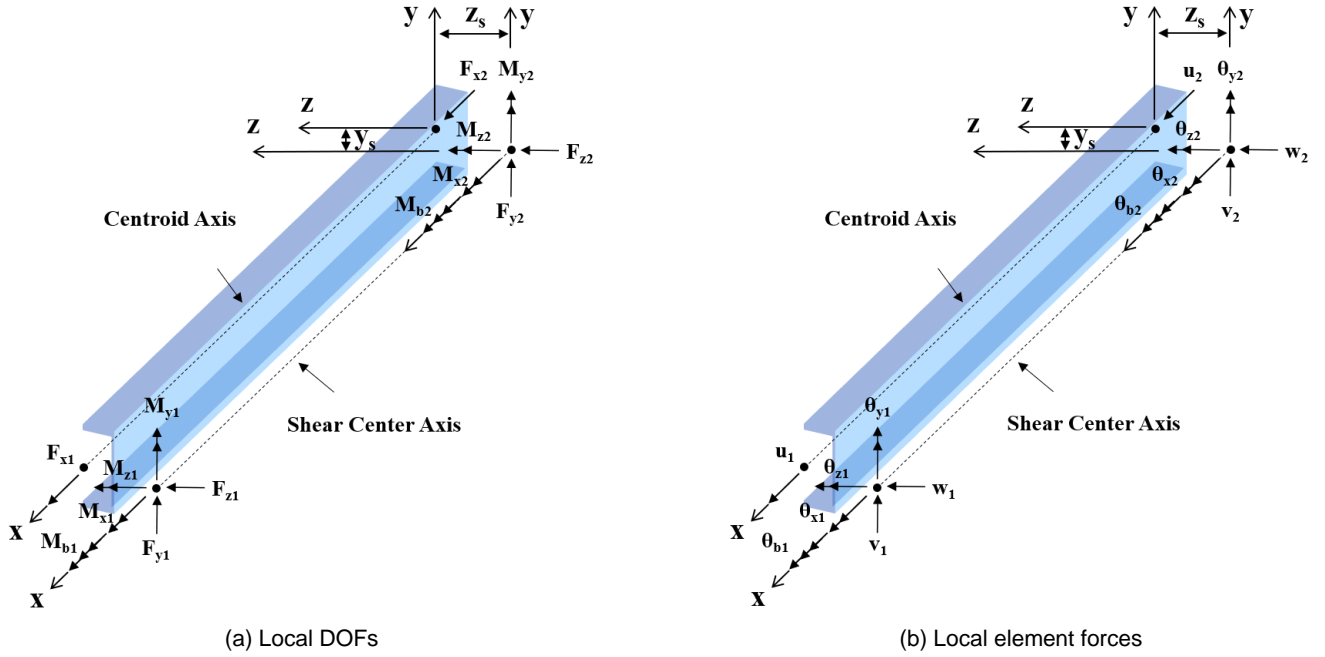


Figure 5 Line-element used in MASTAN2-v5 with nonsymmetrical section

The detailed derivation procedure for the element formulations can be found in the original papers [7, 16]. The equilibrium conditions are established at the element nodes and the deflection shapes within the element are described by the shape functions given by McGuire et al [18]. The strain is then defined by referring to the shape function, and the total strain energy is computed and simplified by ignoring some high-order items, which is given by,

$$\begin{aligned}
 U = & \frac{1}{2} \int_0^L \left[EA \left(\frac{\partial \psi_x(x)}{\partial x} \right)^2 + EI_w \left(\frac{\partial^2 \psi_w(x)}{\partial x^2} \right)^2 + EI_v \left(\frac{\partial^2 \psi_v(x)}{\partial x^2} \right)^2 \right. \\
 & \left. + EI_\omega \left(\frac{\partial^2 \psi_\omega(x)}{\partial x^2} \right)^2 + GJ \left(\frac{\partial \psi_\theta(x)}{\partial x} \right)^2 \right] dx \\
 & + \frac{1}{2} \int_0^L P \left[\left(\frac{\partial \psi_x(x)}{\partial x} \right)^2 + \left(\frac{\partial \psi_w(x)}{\partial x} \right)^2 \right] dx + \frac{1}{2} \int_0^L P r^2 \left(\frac{\partial \psi_\theta(x)}{\partial x} \right)^2 dx + \frac{1}{2} \int_0^L P \left[\begin{matrix} 2v_s \frac{\partial \psi_w(x)}{\partial x} \\ -2w_s \frac{\partial \psi_v(x)}{\partial x} \end{matrix} \right] \frac{\partial \psi_\theta(x)}{\partial x} dx \\
 & + \int_0^L M_{v1} \left[\frac{L-x}{L} \frac{\partial \psi_\theta(x)}{\partial x} \right] \frac{\partial \psi_v(x)}{\partial x} dx - \int_0^L M_{v2} \left[\frac{x}{L} \frac{\partial \psi_\theta(x)}{\partial x} \right] \frac{\partial \psi_v(x)}{\partial x} dx \\
 & + \int_0^L M_{w1} \left[\frac{L-x}{L} \frac{\partial \psi_\theta(x)}{\partial x} \right] \frac{\partial \psi_w(x)}{\partial x} dx - \int_0^L M_{w2} \left[\frac{x}{L} \frac{\partial \psi_\theta(x)}{\partial x} \right] \frac{\partial \psi_w(x)}{\partial x} dx \\
 & + \int_0^L \left[\begin{matrix} V_v \left(\psi_\theta(x) \frac{\partial \psi_w(x)}{\partial x} - \frac{\partial \psi_w(x)}{\partial x} \frac{\partial \psi_v(x)}{\partial x} \right) \\ -V_w \left(\psi_\theta(x) \frac{\partial \psi_v(x)}{\partial x} + \frac{\partial \psi_v(x)}{\partial x} \frac{\partial \psi_w(x)}{\partial x} \right) \end{matrix} \right] dx + \frac{1}{2} \int_0^L M_\theta \beta_\omega \left(\frac{\partial \psi_\theta(x)}{\partial x} \right)^2 dx
 \end{aligned}$$

where, I_v and I_w are the second moments of area about v - and w - axes, respectively; I_ω is the warping constant; J is the torsional rigidity; β_v , β_w , and β_ω are the Wagner

coefficients, which can be computed by an analysis method presented in the reference [16].

The element stiffness matrices are formulated by a second-variation of the total potential energy equation and written as,

$$\delta^2 \Pi = \frac{\delta^2 \Pi}{\delta \zeta_i \delta \zeta_j} \delta \zeta_i \delta \zeta_j = [k_E] \{\Delta u\} - \{\Delta f\} = 0$$

where, $\{\Delta u\}$ and $\{\Delta f\}$ are the incremental displacement and force vectors at the element ends, respectively; and $[k_E]$ is the element stiffness matrix, which is given by,

$$[k_E] = [T]([k_L][\alpha] + [k_G] + [k_U])[T]^T$$

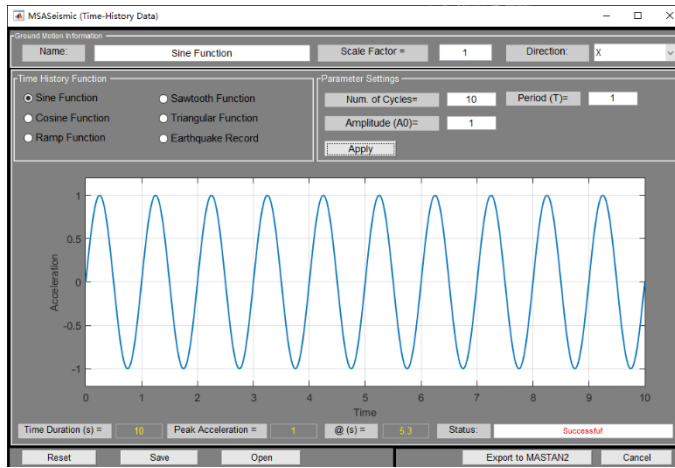
in which, $[k_L]$ is the well-established linear elastic stiffness matrix [3] with reference to the element's x - v - w coordinate system; $[k_G]$ and $[k_U]$ are the geometrical stiffness matrix for symmetrical and nonsymmetrical sections portions, respectively; $[T]$ is the transformation matrix for element local axis to global axis; and $[\alpha]$ is a transformation matrix given in the original paper.

4. Dynamic Frame Analysis in Mastan2-v5

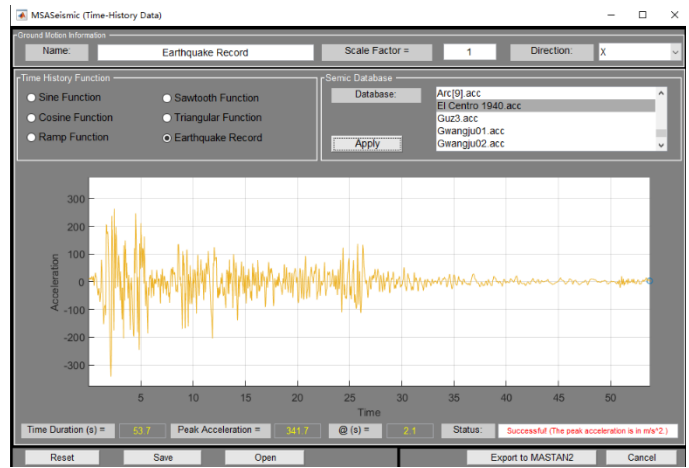
The first-order and second-order time-history analyses algorithms used in this study have been implemented into Mastan2-v5.1 [22], which can directly build the beam-column element analysis model in Mastan-v5.1 [22] and

import the recorded time-acceleration curves or custom excitation load curves into the Msa_Seismic module. The

diagram of the module and the results of the dynamic time-history analysis are shown in Figure 6 below.



(a) MSASeismic module – Sine Function Curve



(b) MSASeismic module – Earthquake Record

Figure 6 MSASeismic Modules within MASTAN2-v5.1

5. Examples

In this section, several examples are provided for investigating the accuracy of the proposed 7DOFs line element (based on the nonsymmetrical section assumption) in solving the dynamic time-history analysis problems.

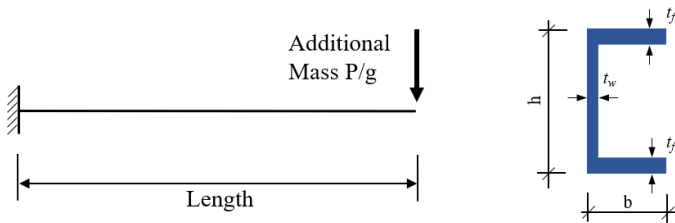


Figure 7. A cantilever beam and the section dimensions

5.1 A cantilever beam under dynamic excitations

This example studies the dynamic responses of a cantilever beam with channel section under the triangular function of excitations. The channel-section cantilever-beam, as shown in Figure 7, has a length of 9.0 m, with dimensions, $h = 300$ mm, $b = 100$ mm, flange plate-thickness ($t_f = 16$ mm), and web thickness ($t_w = 10$ mm). The Young's modulus is 210 Gpa, and Poisson's ratio is 0.3. The member self-weight is not considered in the present dynamic analysis, and a concentrated force of 8 kN is applied as an additional mass to the end of the cantilever beam. Furthermore, since shell finite-element models (SFEM) provide the most accurate results accounting for the aforementioned effects and complexities, a sophisticated SFEM developed by

Abdelrahman et al. [19], as shown in Figure 8, is utilized as benchmark results.

As a sequence, the cantilever beam is subjected to triangular time-history function, as shown in Figure 9. Accordingly, the dynamic responses (i.e. vertical displacement vs time curves) of the cantilever beam under the triangular function excitation are shown in Figure 10. It can be clearly observed that the proposed method employed the line-element with nonsymmetrical section is perfectly matching with the sophisticated SFEM, while the line-element with symmetrical section over-predicts or under-predicts the dynamic response. It can be expected that the dynamic response of symmetrical and nonsymmetrical section members will be far different when they subjected to complex earthquakes, besides if the dominant buckling mode is a flexural-torsional mode.

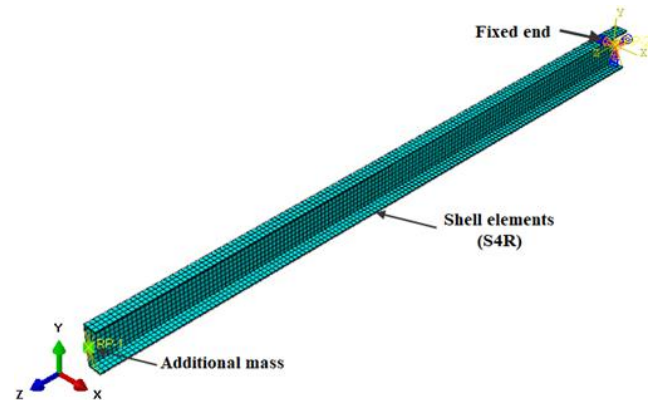


Figure 8. ABAQUS shell finite-element model (SFEM)

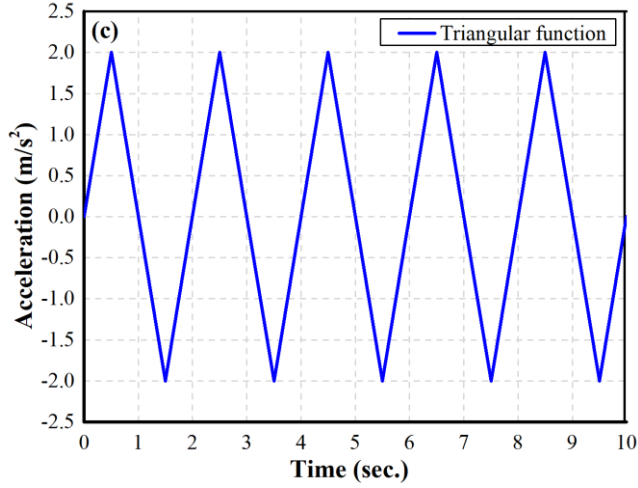


Figure 9. Triangular function

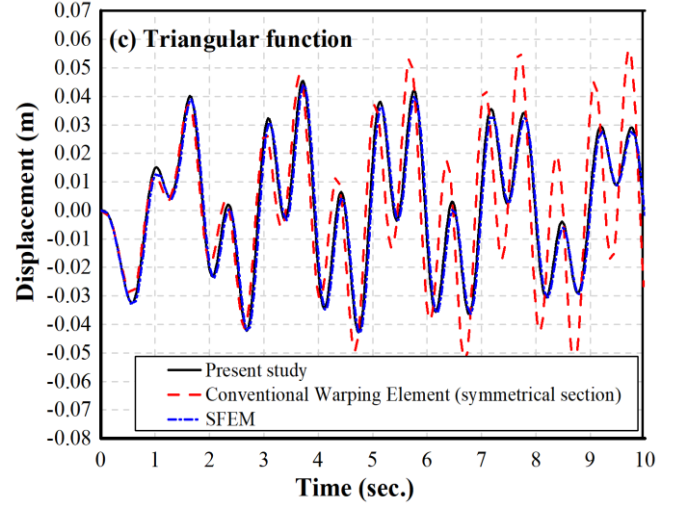


Figure 10. Dynamic response of cantilever beam under dynamic excitations

5.2 An individual column under seismic excitations

This example presents the time-history response of a channel section steel column with a lumped mass at its top under the seismic excitations. The section is C250x30, and the dimensions are shown in Figure 11. The column length is 2000mm, and the Young's modulus and the poisson's ratio are 210GPa and 0.3, respectively. The boundary conditions of this channel column are fixed at one end and free at the other, in which a concentrated force of 15kN is applied as an additional mass. The model is shown schematically in Figure 11. This example focuses on generating the dynamic responses of the channel column under the 1940 EI Centro and the 1971 San Fernando ground excitations (Figure 12) using different line elements, i.e, the nonsymmetric warping 7 DOFs, the conventional symmetric 7 DOFs and the 6DOFs line elements. The time vs. displacements and the time vs. accelerations of the column under two seismic excitations are given in Figure 13.

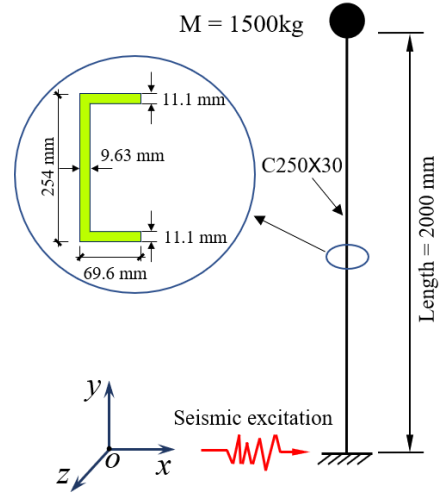
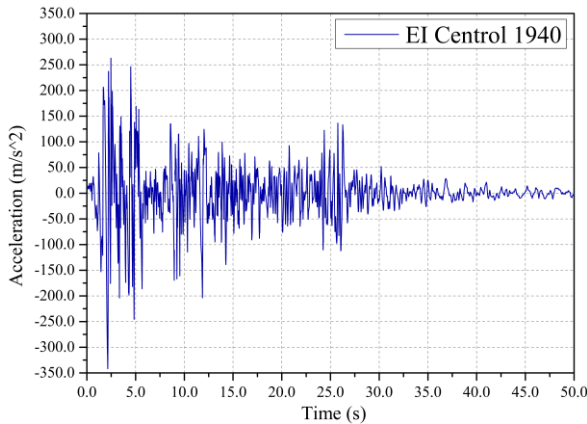
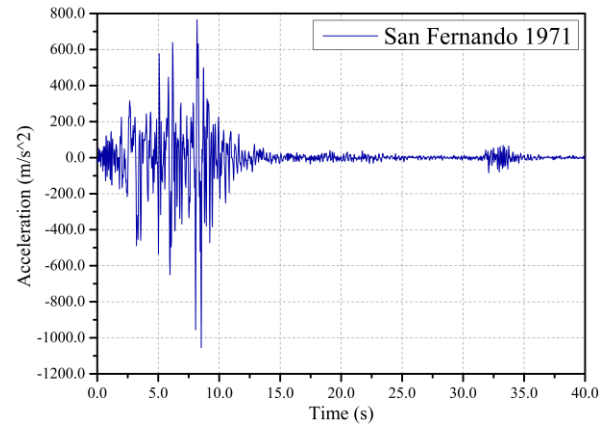


Figure 11. Boundary conditions of individual column

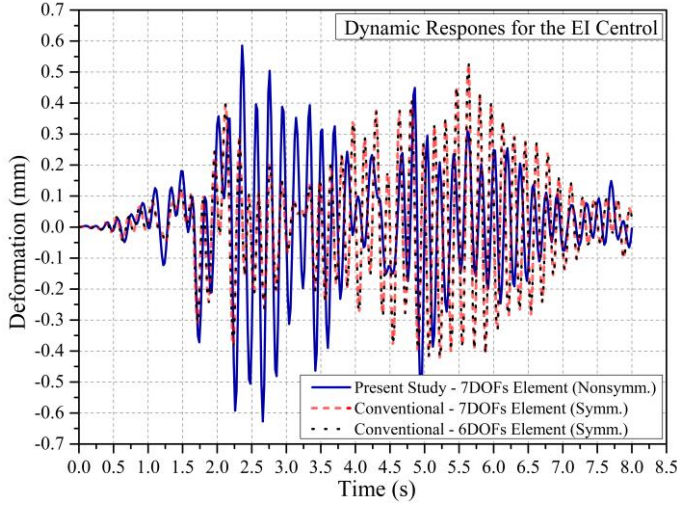


(a) 1940 EI Centro

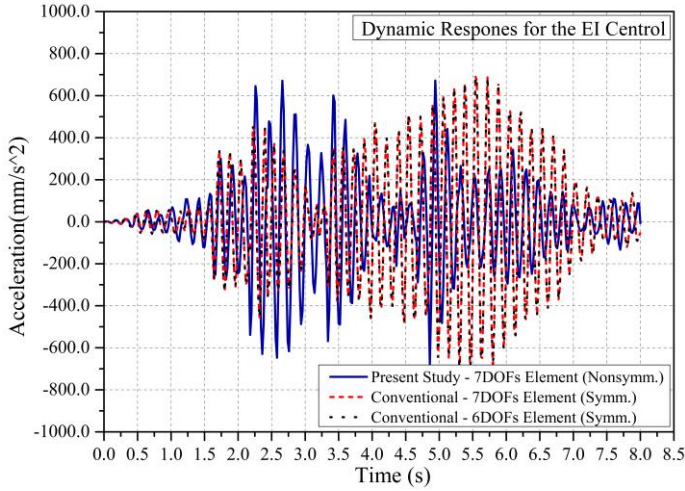


(b) 1971 San Fernando

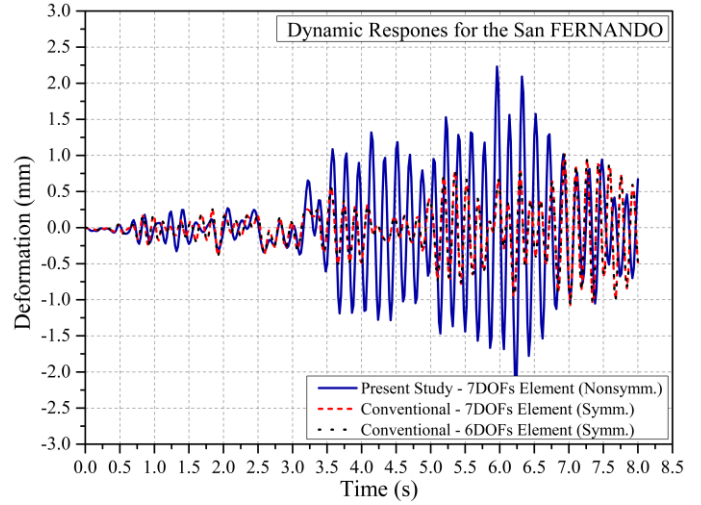
Figure 12. Seismic exications



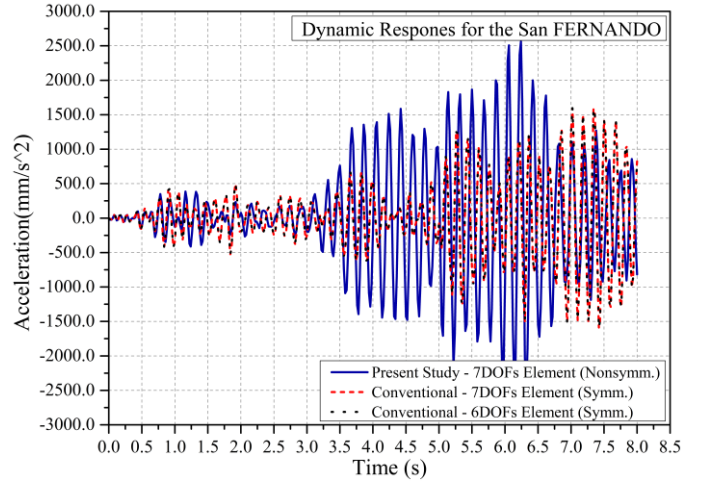
(a) Time-history deflection at the EI-Centro wave



(c) Time-history acceleration at the EI-Centro wave



(b) Time-history deflection at the San Fernando wave



(d) Time-history acceleration at the San Fernando wave

Figure 13. Dynamic response analysis results of the individual columns

5.3 An upright frame under seismic excitations

In this example, the second-order dynamic time history analysis is performed for the steel rack uprights frame. The geometry of the upright frame is shown in Figure 14, with 1000kg additional mass placed at the top of each column. The Young's modulus and Poisson's ratio is 210Gpa and 0.3, respectively. The reduced thickness method is used to consider the perforations on the upright columns. The cross-sectional dimensions of the columns and the diagonal brace are plotted in Figure 15. The boundary conditions at the base of the upright are fixed. The seismic excitation direction is perpendicular to the column and in the plane of the upright frame. The time acceleration curves of the earthquake are taken from the 1940 El Centro and the 1971 San Fernando earthquakes. In this model, the diagonal braces are semi-rigidly connected to the column, details of which can be found in [25].

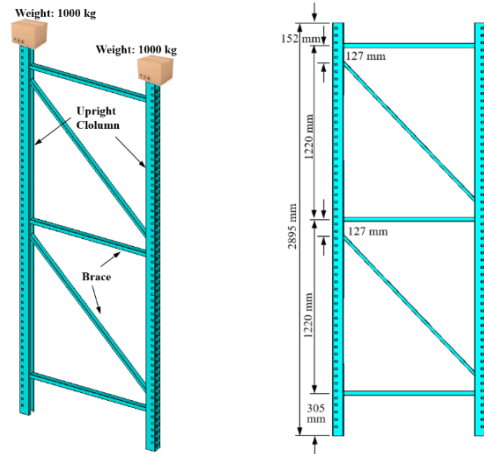


Figure 14. Frame geometry

The analysis results from three different types of line elements are given as shown in Figure 16. From the comparison results, the obvious differences are noted, which indicates the importance of considering the Wagner effect as well as the noncoincident of the shear center and the centroid for the analysis of mono-symmetrical section columns. These analysis results will be useful for revealing the dynamic responses of the frame under seismic excitations.

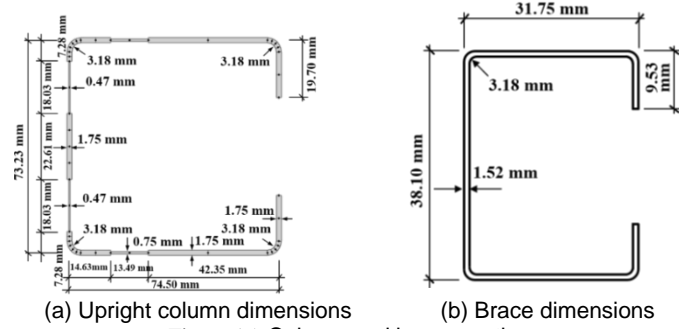
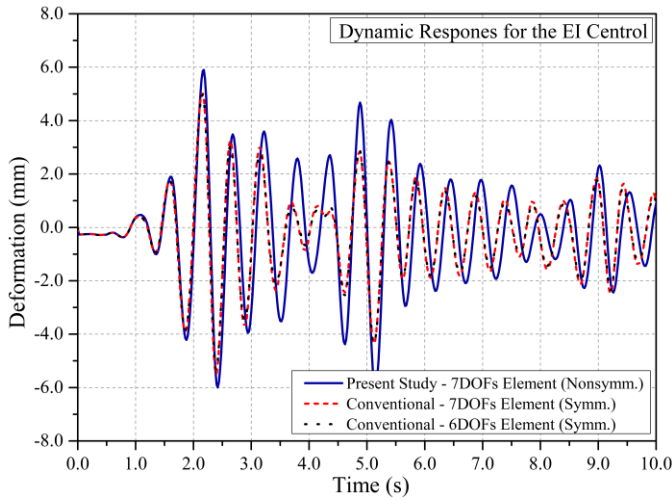
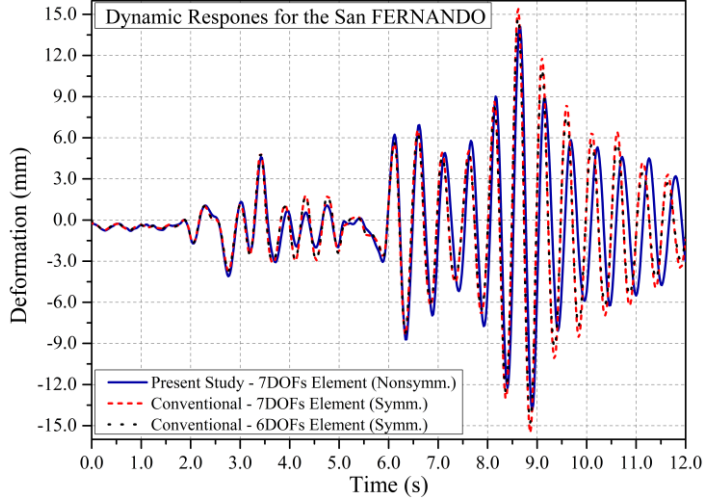


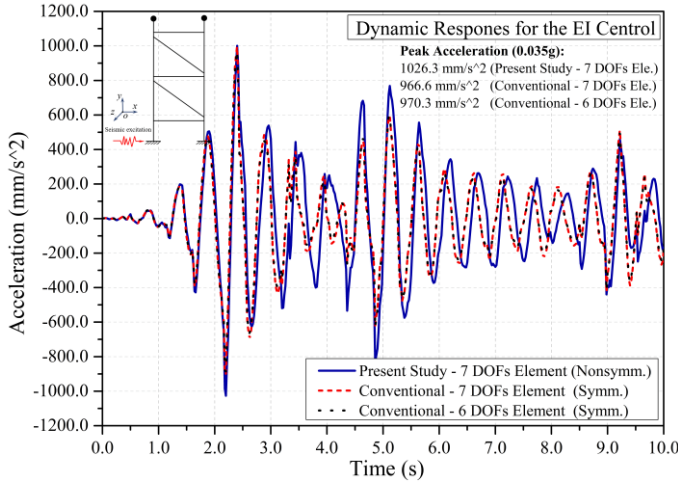
Figure 15. Column and brace section



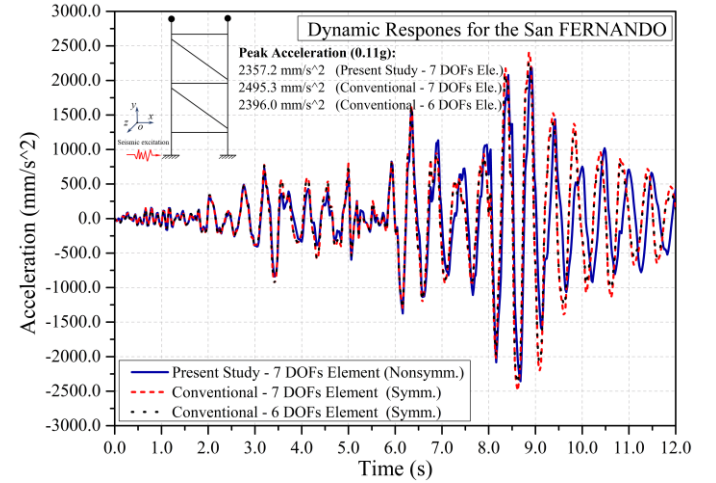
(a) Time-history deflection at the EI-Centro wave



(b) Time-history deflection at the San Fernando wave



(c) Time-history acceleration at the EI-Centro wave



(d) Time-history acceleration at the San Fernando wave

Figure 16. Dynamic response analysis results of the upright frame

5.4 A five-story pallet rack under seismic excitations

In this example, the second-order dynamic analysis is performed for a five-story pallet rack under seismic excitations. The overall structure of the steel rack is shown in Figure 17, and the structural dimensions are shown in

Figure 18. The Young's Modulus and Poisson's ratio are 210Gpa and 0.3, respectively. A uniform load of 637.5 kg/m was distributed across the rack beams to simulate the actual steel rack frame loading conditions when subjected to seismic attacks. The connections of braces to columns and

beams to columns are modeled as semi-rigid joints, as described in [25]. Besides, the column bases are fixed.

The analysis results are given in Figure 19, and the results from different line elements are compared.

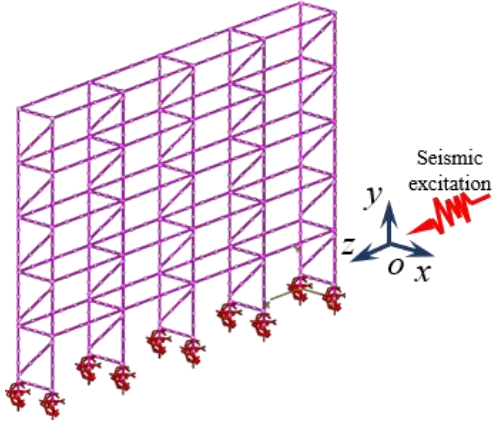


Figure 17. Computer Model

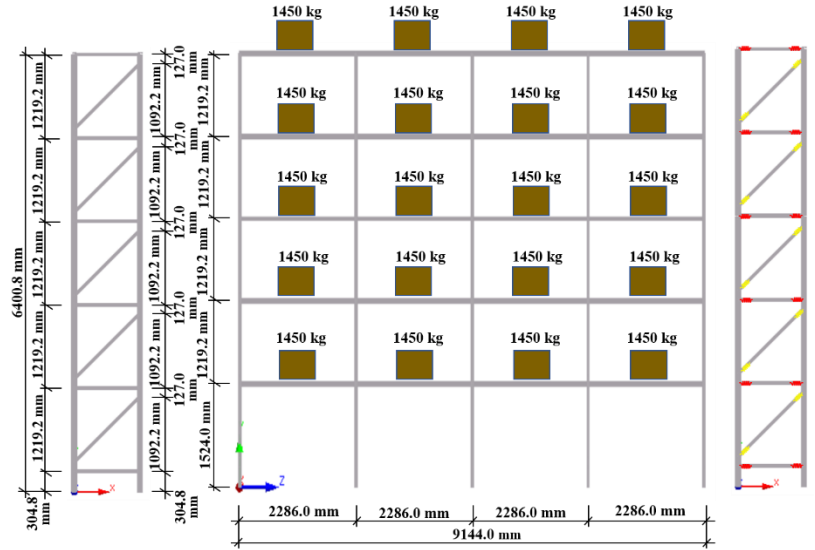
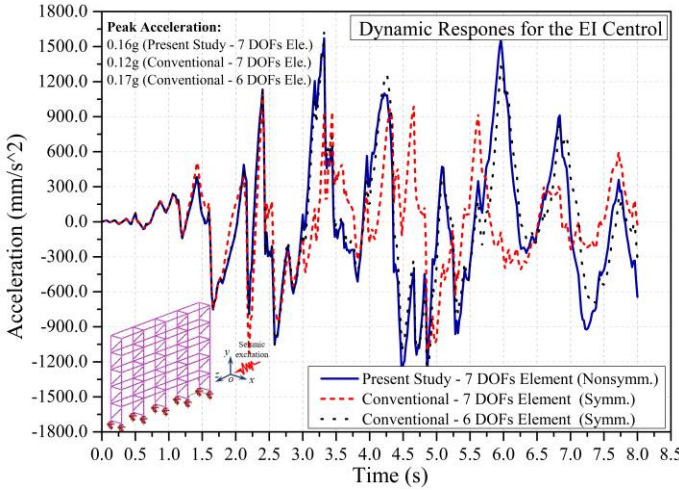
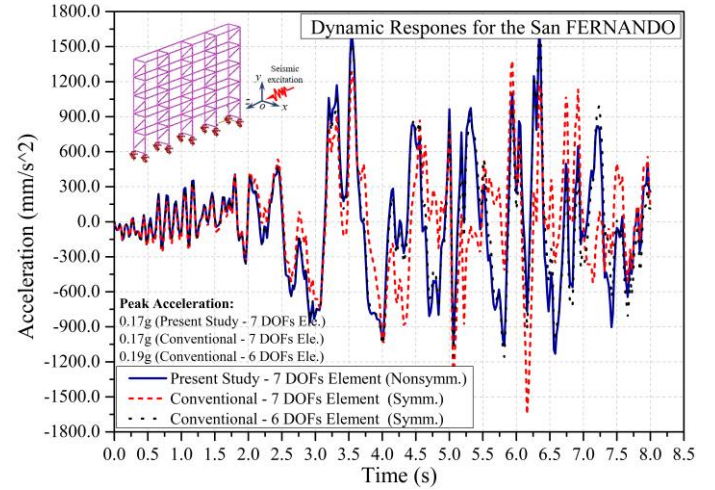


Figure 18. Dimensions of the five-story pallet rack



(a) Time-history acceleration under the EI-Centro earthquake



(b) Time-history acceleration under the San Fernando earthquake

Figure 19. Dynamic analysis results of the five-story pallet rack

6. Conclusion

The present research studies the dynamic time-history responses of the steel storage rack system with perforated cold-formed steel columns and braces under seismic excitations, where the efficient line element frame analysis method within MASTAN2-v5.1 [22] has been introduced. The numerical algorithms, including mathematical derivations of the element formulations, are given in brief. A simple but effective method for considering perforations on the steel column is proposed by reducing the steel plate thickness. Validation examples are given, where the numerical method using shell elements are employed to

generate the benchmark solutions. The common industrial rack structures are analyzed for evaluating their dynamic responses under two typical seismic excitations, providing useful information for the successful applications in high seismic intensity regions.

7. Acknowledgments

The second author would like to express his gratitude to Sun Yat-Sen University on the “Early Research Career Scheme Grant (76140-18831105)”.

References

- [1] A. Firouziyanhaji, A. Saleh, and B. Samali, STABILITY ANALYSIS OF STEEL STORAGE

- RACK STRUCTURES, in 23rd Australasian Conference on the Mechanics of Structures and Materials (ACMSM23). 2014: Byron Bay, Australia, 9-12 December 2014, S.T. Smith (Ed.).
- [2] Lingfeng Yin, Gan Tang, Zhanjie Li, and Min Zhang, Responses of cold-formed steel storage racks with spine bracings using speed-lock connections with bolts II: Nonlinear dynamic response history analysis. *Thin-Walled Structures* [J], 2018. **125**: p. 89-99.
- [3] Barry J. Davidson and Anthony P. McBride, *Design Recommendations for the Improvement of the Seismic Performance of Steel Storage Racks*, in Proceedings of the Ninth Pacific Conference on Earthquake Engineering Building an Earthquake-Resilient Society. 2011: 14-16 April, 2011, Auckland, New Zealand.
- [4] F. Bleich, Buckling strength of metal structures. McGraw-Hill, 1952.
- [5] S.L. Chan and S. Kitipornchai, Geometric nonlinear analysis of asymmetric thin-walled beam-columns. *Engineering Structures* [J], 1987. 9(4): p. 243-254.
- [6] M.A. Bradford and H.R. Ronagh, Generalized elastic buckling of restrained I-Beams by FEM. *Journal of Structural Engineering* [J], 1997. 122(12): p. 1631-1637.
- [7] W. McGuire, R.H. Gallagher, and R.D. Ziemian, Matrix structural analysis. [J], 2000.
- [8] F. Mohri, A. Brouki, and J. Roth, Theoretical and numerical stability analyses of unrestrained monosymmetric thin-walled beams. *Journal of Constructional Steel Research* [J], 2003. 59(1): p. 63-90.
- [9] K.J. Rasmussen, X. Zhang, and H. Zhang, Beam-element-based analysis of locally and/or distortionally buckled members: theory,. *Thin-Walled Structures* [J], 2016. 98: p. 285-292.
- [10] Xi Zhang, Kim J. R. Rasmussen, and Hao Zhang, Beam-element-based analysis of locally and/or distortionally buckled members: Application. *Thin-Walled Structures* [J], 2016. **95**: p. 127-137.
- [11] Si-Wei Liu, Ronald D. Ziemian, Liang Chen, and Siu-Lai Chan, Bifurcation and large-deflection analyses of thin-walled beam-columns with non-symmetric open-sections. *Thin-Walled Structures* [J], 2018. **132**: p. 287-301.
- [12] XianZhong Zhao, Chong Ren, and Ru Qin, An experimental investigation into perforated and non-perforated steel storage rack uprights. *Thin-Walled Structures* [J], 2018. **112**: p. 159-172.
- [13] Nadia Baldassino, Claudio Bernuzzi, Arturo di Gioia, and Marco Simoncelli, An experimental investigation on solid and perforated steel storage racks uprights. *Journal of Constructional Steel Research* [J], 2019. **155**: p. 400-425.
- [14] Miquel Casafont, Maria Magdalena Pastor, Francesc Roure, and Teoman Peköz, An experimental investigation of distortional buckling of steel storage rack columns. *Thin-Walled Structures* [J], 2011. **49**(8): p. 933-946.
- [15] Miquel Casafont, Francesc Roure, Magdalena Pastor, Jordi Bonada, and Teoman Peköz, *Distortional buckling test for steel storage rack columns*, in *Proceedings of the Institution of Civil Engineers - Structures and Buildings*. 2013. p. 392-402.
- [16] Cristopher D. Moen and B. W. Schafer, Experiments on cold-formed steel columns with holes. *Thin-Walled Structures* [J], 2008. **46**(10): p. 1164-1182.
- [17] M. Casafont, M.M. Pastor, F. Roure, J. Bonada, and T. Pekoz, An investigation on the design of steel storage rack column via the direct strength method. *Journal of Constructional Steel Research* [J], 2013. **139**(5): p. 669-679.
- [18] Miquel Casafont, Magdalena Pastor, Jordi Bonada, Francesc Roure, and Teoman Peköz, Linear buckling analysis of perforated steel storage rack columns with the Finite Strip Method. *Thin-Walled Structures* [J], 2012. **61**: p. 71-85.
- [19] B. W. Schafer, CUFSM 5.01—Finite strip buckling analysis of thin-walled members. Baltimore, USA: Department of Civil Engineering, Johns Hopkins University [J], 2018.
- [20] Si-Wei Liu, Ronald D. Ziemian, Liang Chen, and Siu-Lai Chan, Bifurcation and large-deflection analyses of thin-walled beam-columns with non-symmetric open-sections. *Thin-Walled Structures* [J], 2018. **132**: p. 287-301.
- [21] Si-Wei Liu, Wen-Long Gao, and Ronald D. Ziemian, Improved line-element formulations for the stability analysis of arbitrarily-shaped open-section beam-columns. *Thin-Walled Structures* [J], 2019. **144**.
- [22] Ronald D. Ziemian, W McGuire, and Si-Wei Liu, MASTAN2 v5.1., 2020.
- [23] Ronald D. Ziemian and W McGuire, Modified tangent modulus approach, a contribution to plastic hinge analysis. *Journal of Structural Engineering* [J], 2002. **128**(10): p. 1301.
- [24] A.H.A. Abdelrahman, Y.P. Liu, S.W. Liu and S.L. Chan (2020). Simulation of thin-walled members with arbitrary-shaped cross-sections for static and dynamic analyses", *International Journal of Structural Stability and Dynamics*, <https://doi.org/10.1142/S021945542050128X>
- [25] Si-Wei Liu, Teoman Pekoz, Wen-Long Gao, Ronald D. Ziemian and James Crews, Frame Analysis and Design of Industrial Rack Structures with Perforated Cold-Formed Steel Columns. currently under review *Thin-Walled Structures* [J].2020